Int. J. Dev. Biol. 56: 393-402 (2012)
doi: 10.1387/ijdb.113333ct

THE INTERNATIONAL JOURNAL OF DEVELOPMENTAL BIOLOGY
www.intjdevbiol.com

Identification and characterization of *Xenopus kctd15*, an ectodermal gene repressed by the FGF pathway

CHIKA TAKAHASHI[1], TOSHIYASU SUZUKI[1], EISUKE NISHIDA[1,2] and MORIOH KUSAKABE*[,1,2]

[1]*Department of Cell and Developmental Biology, Graduate School of Biostudies, Kyoto University, Kyoto, Japan and* [2]*JST, CREST, Tokyo, Japan*

ABSTRACT The FGF pathway regulates a variety of developmental processes in animals through activation and/or repression of numerous target genes. Here we have identified a *Xenopus* homolog of *potassium channel tetramerization domain containing 15 (KCTD15)* as an FGF-repressed gene. *Kctd15* expression is first detected at the gastrula stage and gradually increases until the tadpole stage. Whole-mount *in situ* hybridization reveals that the spatial expression of *kctd15* is tightly regulated during early embryogenesis. While *kctd15* is uniformly expressed throughout the presumptive ectoderm at the early gastrula stage, its expression becomes restricted to the non-neural ectoderm and is excluded from the neural plate at the early neurula stage. At the mid-neurula stage, *kctd15* shows a more restricted distribution pattern in regions that are located at the anterior, lateral or medial edge of the neural fold, including the preplacodal ectoderm, the craniofacial neural crest and the prospective roof plate. At the tailbud stage, *kctd15* expression is mainly detected in neural crest- or placode-derived tissues that are located around the eye, including the mandibular arch, trigeminal ganglia and the olfactory placode. FGF represses *kctd15* expression in ectodermal explants, and the inhibition of FGF receptor with a chemical compound dramatically expands the region expressing *kctd15* in whole embryos. Dorsal depletion of kctd15 in *Xenopus* embryos leads to bent axes with reduced head structures, defective eyes and abnormal somites, while ventral depletion causes defects in ventral and caudal morphologies. These results suggest that *kctd15* is an FGF-repressed ectodermal gene required for both dorsal and ventral development.

KEY WORDS: *kctd15, Xenopus, FGF, ectoderm*

Fibroblast growth factor (FGF) is a key secreted factor that controls cell proliferation, cell differentiation and various developmental processes in animals (Böttcher and Niehrs, 2005; Thisse and Thisse, 2005). In early *Xenopus* development, FGF and its major downstream signaling pathway, the Ras/MAPK pathway, play an essential role in mesoderm formation and neural induction (De Robertis and Kuroda, 2004; Heasman, 2006). The FGF/Ras/MAPK pathway functions through transcriptional activation and/or repression of numerous but specific target genes, which include a wide variety of transcriptional factors, regulators of the intracellular signal transduction pathway and secreted factors (Chung *et al*., 2004; Böttcher and Niehrs, 2005; Thisse and Thisse, 2005; Branney *et al*., 2009). In this study, we have identified a *Xenopus* homolog of *potassium channel tetramerization domain containing 15* (*KCTD15*) as an FGF-repressed gene.

KCTD15 is a member of the KCTD family sharing a common N-terminal domain, the potassium channel tetramerisation domain (also known as the T1 domain) that is homologous to the cytoplasmic domain of voltage-gated potassium channels. This domain is a close relative of the BTB (Broad-Complex, Tramtrack and Bric a brac)/POZ (poxvirus and zinc finger) domain, which is a major protein-protein interaction motif found in viruses and throughout eukaryotes (Perez-Torrado *et al*., 2006). Although the role of the KCTD family members remains largely unknown, several studies suggest that they are involved in various biological processes. For example, it has been shown that *KCTD11* is deleted in human medulloblastoma and negatively regulates the Hedgehog signaling pathway by ubiquitin-mediated proteolysis (Di Marcotullio *et al*., 2004; Canettieri *et al*., 2010). Also, KCTD8, 12 and 16 have been identified as auxiliary $GABA_B$ receptor subunits that determine the

Abbreviations used in this paper: FGF, fibroblast growth factor; KCTD, potassium channel tetramerization domain.

***Address correspondence to:** Morioh Kusakabe. Department of Cell and Developmental Biology, Graduate School of Biostudies, Kyoto University, Sakyo-ku, Kyoto 606-8502, Japan. Tel: +81-75-753-4232. Fax: +81-75-753-4235. E-mail: morioh@lif.kyoto-u.ac.jp

Accepted: 16 March 2012. *Final, author-corrected PDF published online:* 15 June 2012. *Edited by:* Sally Dunwoodie

ISSN: Online 1696-3547, Print 0214-6282
© 2012 UBC Press
Printed in Spain

pharmacology and kinetics of the receptor response (Schwenk *et al.*, 2010; Bartoi *et al.*, 2010).

KCTD15 genes are present in human and other vertebrates (also see Fig. 1 C,D), and previous genome-wide association studies have shown that human *KCTD15* is one of candidate genes that are associated with adult obesity risk (Thorleifsson *et al.*, 2009; Willer *et al.*, 2009). Moreover, it has been recently shown that zebrafish homologs of *KCTD15* inhibit neural crest formation by interfering with the Wnt/beta-catenin signaling pathway (Dutta and Dawid, 2010). These findings thus raise the possibility that KCTD15 is a commonly used signaling molecule that regulates multiple biological phenomena in vertebrates. In this study, we describe the developmental expression and function of *Xenopus kctd15*, thereby providing more insights into the role of KCTD15 in vertebrates.

Results

Xenopus kctd15 *is a novel FGF-repressed gene*

Through a preliminary microarray experiment, in which the expression profile of *Xenopus* ectodermal explants treated with FGF was compared with that of untreated control explants (Kusakabe and Nishida, unpublished data), we found that a *Xenopus* homolog of *KCTD15* (*kctd15*) is a potential candidate for one of FGF-repressed genes. Real-time quantitative RT-PCR analysis indicated that the expression level of *kctd15* was reduced to about half by FGF in *Xenopus* ectodermal explants (Fig. 1A). Ras is an essential component of the FGF signaling pathway (Böttcher and Niehrs, 2005; Thisse and Thisse, 2005). Overexpression

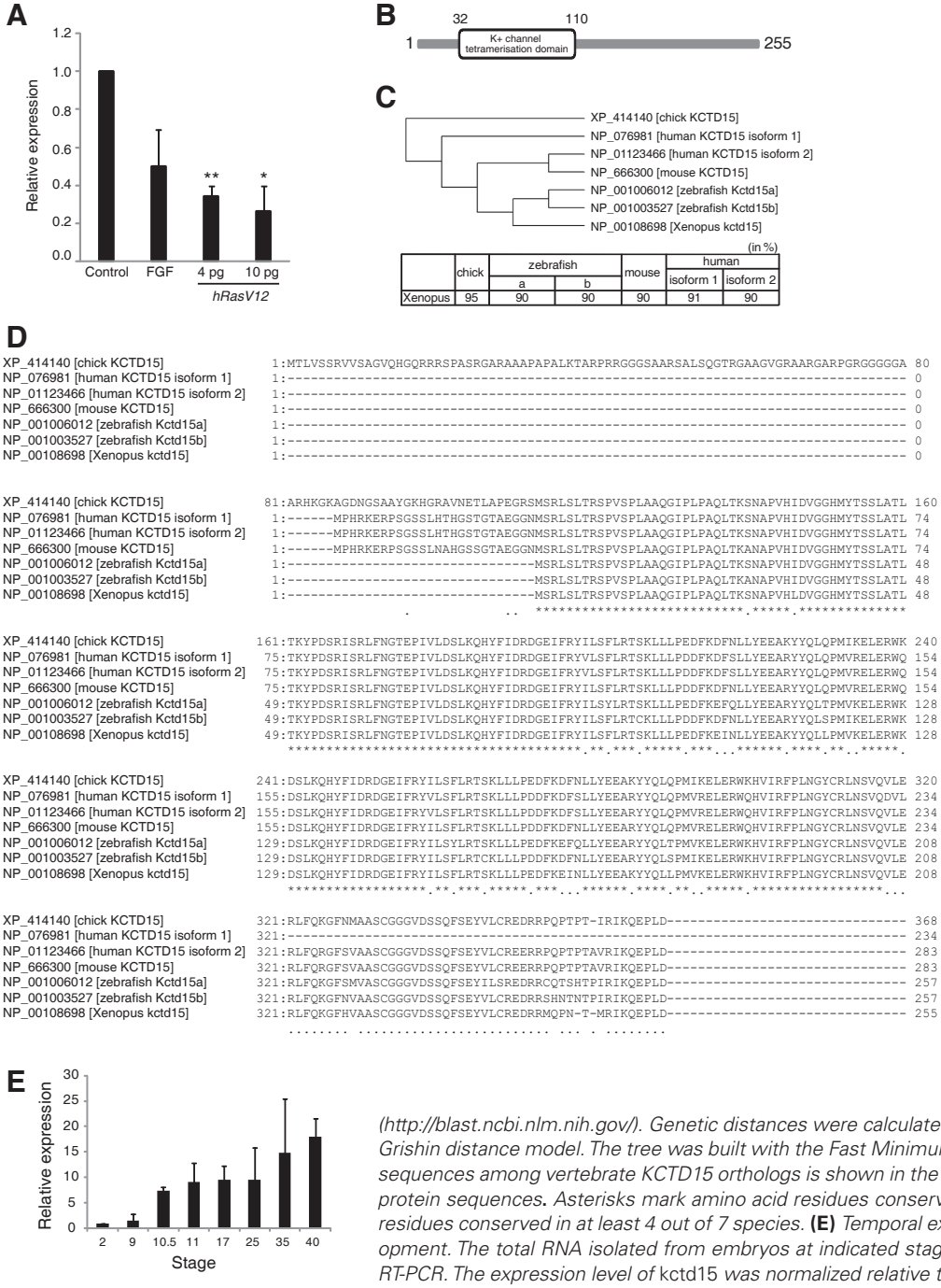

Fig. 1. Evolutionary conservation of *Xenopus kctd15,* a novel FGF-repressed gene. (A) Xenopus *Kctd15 expression is repressed by FGF or RasV12 in ectodermal explants.* hRasV12 *mRNA was injected into the animal poles of four-cell stage embryos. Ectodermal explants derived from uninjected or injected embryos were left untreated or treated with 100 ng/ml FGF. At stage 11, explants were harvested for RNA preparation. The expression level of* kctd15 *was determined by real-time quantitative RT-PCR and normalized relative to that of* ef1a. *Shown is the average of two independent experiments. The error bar represents the standard deviation (SD). Significant differences are marked by asterisks (*$p < 0.05$, **$p < 0.01$, unpaired t test). P values versus control were as follows: 0.067 for FGF-treated explants, 0.0030 for* hRasV12 *mRNA (4 pg)-injected explants, and 0.016 for* hRasV12 *mRNA (10 pg)-injected explants.* **(B)** *Schematic representation of* Xenopus *kctd15 protein.* Xenopus *kctd15 consists of 255 amino acids and has the potassium channel tetramerization domain at the N-terminus.* **(C)** *A phylogenetic tree of vertebrate KCTD15 proteins. The tree was drawn by the BLAST TreeView Widget (http://blast.ncbi.nlm.nih.gov/). Genetic distances were calculated from the aligned sequences by using the Grishin distance model. The tree was built with the Fast Minimum Evolution method. Identity of amino acid sequences among vertebrate KCTD15 orthologs is shown in the table.* **(D)** *Alignment of vertebrate KCTD15 protein sequences***.** *Asterisks mark amino acid residues conserved in all species. Periods mark amino acid residues conserved in at least 4 out of 7 species.* **(E)** *Temporal expression of* Xenopus kctd15 *in early development. The total RNA isolated from embryos at indicated stages was subjected to real-time quantitative RT-PCR. The expression level of* kctd15 *was normalized relative to that of* odc. *Shown is the average of two independent experiments. The error bar represents the standard deviation (SD).*

of a constitutively active mutant of human *Ras* (*hRasV12*) led to a more significant decrease in the expression level of *kctd15* than that observed in FGF-treated explants (Fig. 1A). These results suggest that the FGF/Ras signaling pathway negatively regulates *kctd15* expression in *Xenopus* embryos. *Xenopus* kctd15 protein consists of 255 amino acids and has the potassium channel tetramerization domain (Pfam accession number PF02214), a close relative of the BTB domain (Pfam accession number PF00651) (Fig. 1B). The potassium channel tetramerization domain and the BTB domain constitute the BTB superfamily (superfamily cluster accession number cl02518) that is defined in the NCBI conserved domain database. *Xenopus* kctd15 protein shows 90-95% amino acid identity with its orthologs in other vertebrate species ranging from fish to human (Fig. 1 C,D). This high degree of sequence conservation suggests that KCTD15 plays a fundamental role in vertebrates.

Temporal and spatial expression of Xenopus kctd15

We next examined the temporal expression pattern of *Xenopus kctd15* during early embryogenesis by real-time quantitative RT-PCR analysis. Maternal transcripts were not detected (Fig. 1E). The expression was first detected at the early gastrula stage (stage 10.5) and gradually increased until the tadpole stage (stage 40) (Fig. 1E). This result indicates that the expression level of *kctd15* is regulated during embryogenesis. We then analyzed the spatial expression pattern of *kctd15* by whole-mount *in situ* hybridization. At the early gastrula stage (stage 10.5), *kctd15* transcripts were uniformly present throughout the presumptive ectoderm in the animal region, and no obvious expression was detected in the vegetal region (Fig. 2 A-C). At the early neurula stage (stage 14), *kctd15* expression became restricted to the non-neural ectoderm and was excluded from the neural plate (Fig. 2 D-G). At the mid-neurula stage (stage 16), *kctd15* showed a more restricted distribution pattern in specific areas that are located at the anterior, lateral or medial edge of the neural fold (Fig. 2 H-J). The most prominent expression was found within the presumptive neural crest (nc) lying just lateral to the neural plate (Fig. 2J). This region was roughly divided into two distinct subregions (Fig. 2J). The anterior one may be a part of the putative craniofacial neural crest including the mandibular crest, and the posterior one may be a part of the putative trunk neural crest (Sadaghiani and Thiébaud, 1987). Also, *kctd15* expression was detected in the narrow crescent-shaped region surrounding the anterior neural plate, which corresponds to the preplacodal ectoderm (ppe) (Fig. 2H), and the medial edge of the neural fold, which corresponds to the prospective roof plate (rf) (Fig. 2J). At the late neurula stage (stage 18), *kctd15* expression was detected in the neural crest, the roof plate and the olfactory placode (pOl) (Fig. 2 K-M). At the tailbud stage (stage 25), *kctd15* expression was mainly detected in neural crest- or placode-derived tissues that are located around the eye, including the olfactory placode, the mandibular arch (Md), the hyoid arch (Hy), trigeminal ganglia (tg) and the anterodorsal lateral line placode (pAD) (Fig. 2 N-P). Also, the faint expression was detected in the putative pronephric duct (pd) (Fig. 2N). To confirm that *kctd15* is expressed in the neural crest, we performed whole mount double *in situ* hybridiza-

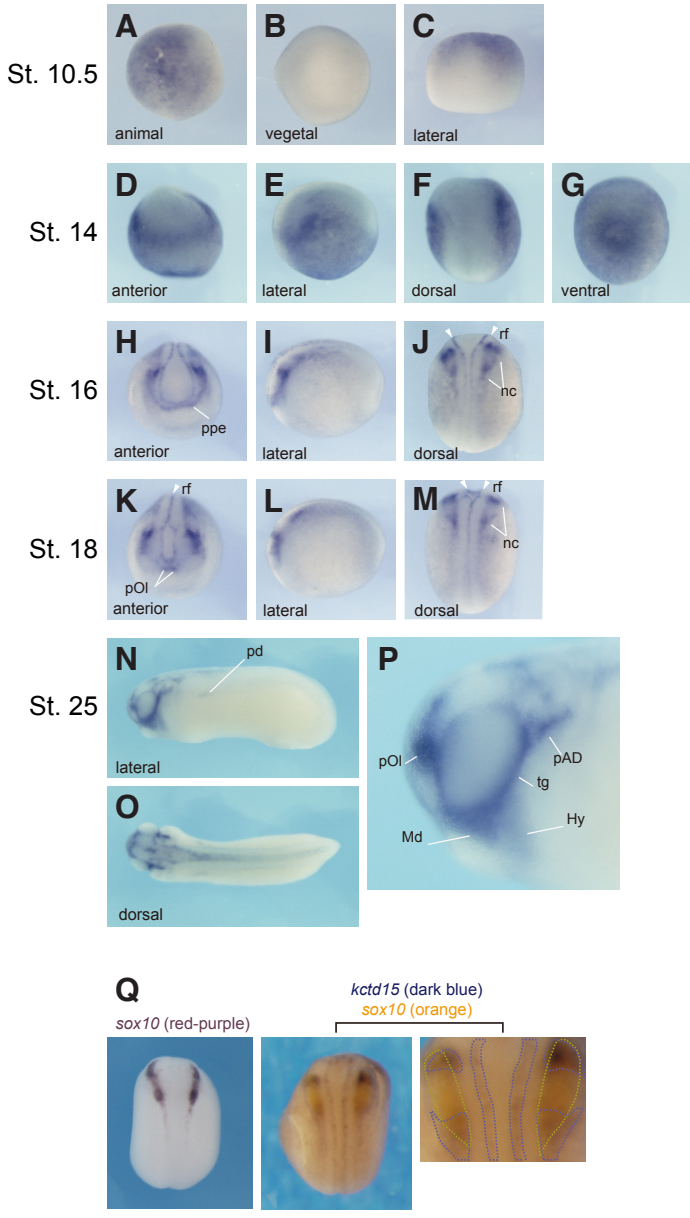

Fig. 2 Spatial expression of *Xenopus kctd15* in early development. *Whole mount* in situ *hybridization against* kctd15 *was performed on embryos from indicated stages. No detectable signal was seen with the sense probe (data not shown).* **(A-C)** *At stage 10.5,* kctd15 *was uniformly expressed throughout the presumptive ectoderm.* **(D-G)** *At stage 14,* kctd15 *expression was detected in the non-neural ectoderm and was excluded from the neural plate. Dorsal is upward in D and E. Anterior is upward in F and G.* **(H-J)** *At stage 16,* kctd15 *expression was detected in the preplacodal ectoderm (ppe), the neural crest (nc) and the roof plate (rf). Dorsal is upward in H and I. Anterior is upward in J.* **(K-M)** *At stage 18,* kctd15 *expression was detected in the neural crest (nc), the roof plate (rf) and the olfactory placode (pOl). Dorsal is upward in K and L. Anterior is upward in M.* **(N-P)** *At stage 25,* kctd15 *expression was detected in the pronephric duct (pd), the mandibular arch (Md), the hyoid arch (Hy), the olfactory placode (pOl), trigeminal ganglia (tg) and the anterodorsal lateral line placode (pAD). Anterior is left.* **(Q)** *Whole mount double* in situ *hybridization against* kctd15 *and* sox10 *was performed on stage 17 embryos (middle and right panels). The right panel is an enlarged view of the middle panel. Dark blue and orange dotted lines mark the* kctd15*-expressing and* sox10*-expressing area, respectively. For reference, single* in situ *hybridization against* sox10 *(red purple) was also performed (the left panel). All panels are dorsal views with anterior to the top.*

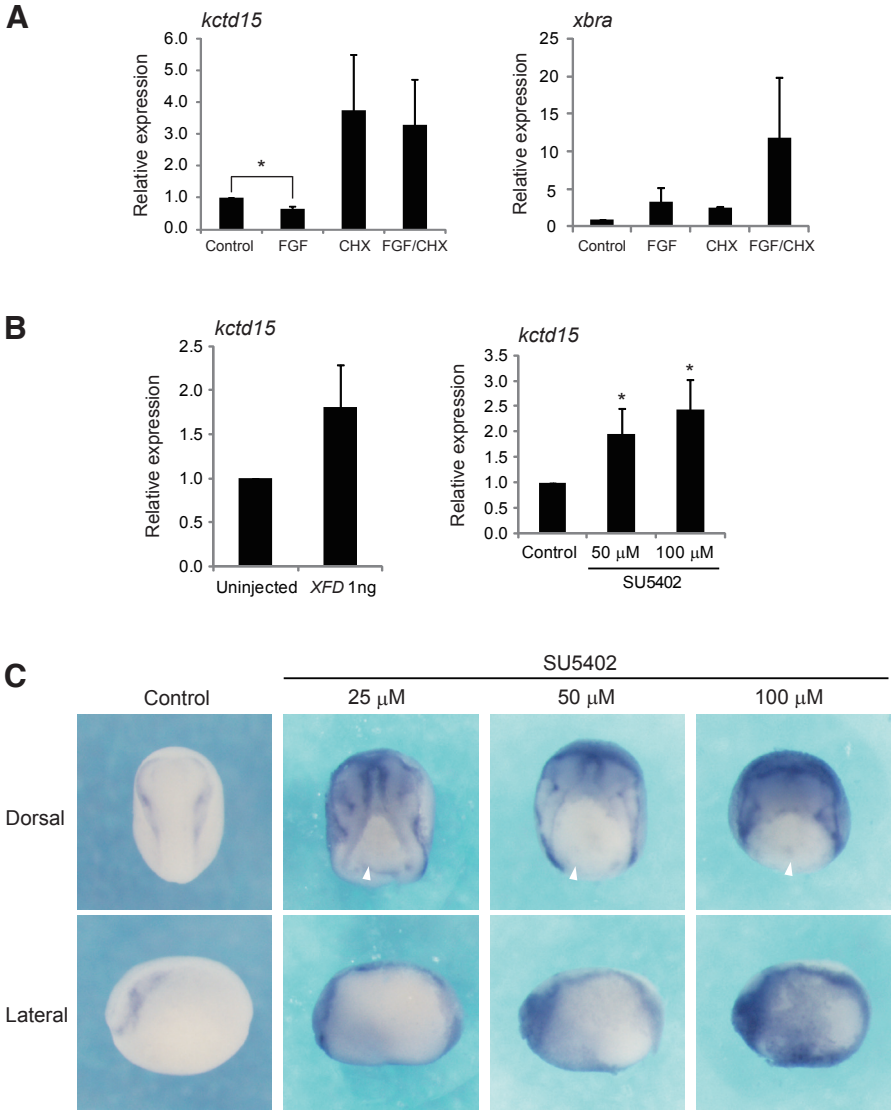

Fig. 3. FGF signaling inhibits *Xenopus kctd15* expression *in vivo*. (A) *FGF represses* kctd15 *expression indirectly. Animal caps were dissected at stage 10.25, treated with FGF (100 ng/ml) for 3 hours in the presence or absence of cycloheximide (CHX; 5 μg/ml), and then harvested for real-time quantitative RT-PCR analysis. Shown is the average of two independent experiments. The error bar represents SD. Significant differences are marked by asterisks (*p < 0.05, unpaired t test). P values (FGF treatment versus no FGF treatment) were as follows: 0.024 for* kctd15 *expression in the absence of CHX, 0.80 for* kctd15 *expression in the presence of CHX, 0.23 for* xbra *expression in the absence of CHX, and 0.24 for* xbra *expression in the presence of CHX.* **(B)** *Inhibition of FGF signaling increases the abundance of* kctd15 *mRNA.* XFD *mRNA (1 ng) was injected into animal poles at 2-cell stage, and injected embryos were harvested at stage 11 for real-time quantitative RT-PCR analysis (left). Embryos were treated with indicated doses of SU5402 at stage 9, and then harvested at stage 11 for real-time quantitative RT-PCR analysis (right). Shown is the average of two (left) or three (right) independent experiments. The error bar represents SD. *P < 0.05, unpaired t test. P values versus control were as follows: 0.14 for* XFD *mRNA-injected embryos, 0.031 for SU5402 (50 μM)-treated embryos, and 0.015 for SU5402 (100 μM)-treated embryos.* **(C)** *Inhibition of FGF signaling dramatically expands the region expressing* kctd15*. Embryos were treated with indicated doses of SU5402 at stage 9, fixed at stage 15, and then subjected for whole mount* in situ *hybridization against* kctd15*. Upper panels show dorsal views with anterior toward the top. Lower panels show lateral views with anterior to the left. White arrowheads indicate unclosed blastopores, which are commonly observed phenotypes caused by inhibition of the FGF pathway (Amaya* et al.*, 1991; Chung* et al.*, 2004).*

tion on stage 17 embryos, and compared the expression pattern of *kctd15* with that of an early neural crest marker *sox10*. The region expressing *kctd15* overlapped with anterior and posterior parts, but not the middle part, of the region expressing *sox10* (Fig. 2Q), indicating that *kctd15* is expressed in specific areas of the neural crest. Our results thus reveal that *kctd15* shows a temporally and spatially regulated expression pattern during early *Xenopus* development.

Xenopus kctd15 *expression is suppressed by FGF signaling* in vivo

In order to investigate whether FGF represses *kctd15* expression directly or indirectly, animal cap explants were dissected from gastrula embryos, and incubated with FGF in the presence or absence of a protein synthesis inhibitor cycloheximide (CHX). The expression level of *kctd15* was then analyzed by real-time quantitative RT-PCR analysis. In the absence of CHX, FGF led to a 34% reduction in the expression level of *kctd15* (Fig. 3A, two left bars in the left graph), while in the presence of CHX, FGF led to only a 12% reduction (Fig. 3A, two right bars in the left graph). As a positive control, we also examined the expression level of *xbra*, an established direct target of FGF (Smith *et al.*, 1991). FGF-dependent increase in *xbra* expression is 2.6-fold in the absence of CHX, while it is 3.6-fold in the presence of CHX (Fig 3A, the right graph), confirming that *xbra* induction by FGF is direct. For unknown reasons, CHX treatment increased basal expression levels of *kctd15* and *xbra*. These results imply that FGF represses *kctd15* expression in an indirect manner that is predominantly dependent on *de novo* protein synthesis.

We next examined whether FGF represses *kctd15* expression *in vivo*. Real-time quantitative RT-PCR analysis indicated that embryos overexpressing *XFD*, a dominant negative form of *Xenopus* FGF receptor 1 (Amaya *et al.*, 1991), exhibited an increase in the amount of *kctd15* mRNA, compared with control embryos (Fig. 3B, left). Moreover, treatment of embryos with a chemical inhibitor of FGF receptor, SU5402, led to a dose-dependent increase in the amount of *kctd15* mRNA (Fig. 3B, right). These results indicate that the FGF pathway controls the amount of *kctd15* mRNA to an adequate level. Also, whole-mount *in situ* hybridization was performed to investigate whether the FGF pathway is responsible for the spatial controlled expression pattern of *kctd15*. SU5402 treatment from the blastula stage onwards dramatically expanded the

region expressing *kctd15* in embryos at the mid-neurula stage (stage 15) with dose dependency: *kctd15* expression restricted to the anterior or anterolateral neural plate border in control embryos while it expanded to the anterior abdomen and the posterior neural plate border in SU5402-treated embryos (Fig. 3C). These results thus strongly suggest that FGF signaling restricts *kctd15* expression *in vivo*.

Xenopus kctd15 *is essential for head and somite development*

To examine the function of *Xenopus kctd15* in early embryonic development by a loss-of-function approach, we designed an antisense morpholino oligonucleotide (MO) against *kctd15*. To check the ability of *kctd15* MO to block translation from *kctd15* mRNA, the combination of *GFP* mRNA plus control MO or *kctd15* MO was co-injected with *kctd15-myc* mRNA, which consisted of the 5'UTR and the coding region of *kctd15* with a myc tag at the C terminus. Immunoblot analysis revealed that *kctd15* MO markedly reduced the protein abundance of kctd15-myc, but not that of GFP (Fig. 4A, two right lanes). Thus, *kctd15* MO is specific and efficient. Control MO or *kctd15* MO was then injected into animal poles of dorsal blastomeres at the four-cell stage, and injected embryos were allowed to develop. At the late tailbud stage, embryos dorsally injected with *kctd15* MO exhibited bent axes with reduced head structures, defective eyes and abnormal somites, whereas embryos injected with control MO were almost normal (Fig. 4 B,C). We classified the phenotypes of MO-injected embryos into three groups according to the extent of defects in head morphologies (Fig. 4D). Thirty-nine percent of *kctd15* MO-injected embryos showed severe phenotypes comprising reduced head structures with no eyes, 61% of those showed milder phenotypes comprising reduced head structures with small eyes, and 0% of those had normal head structures (Fig. 4D). Also, we classified the phenotypes of injected embryos into three groups according to the extent of defects in somite morphologies (Fig. 4E). Thirty percent of *kctd15* MO-injected embryos showed severe phenotypes comprising a decrease in both the dorsoventral length and the

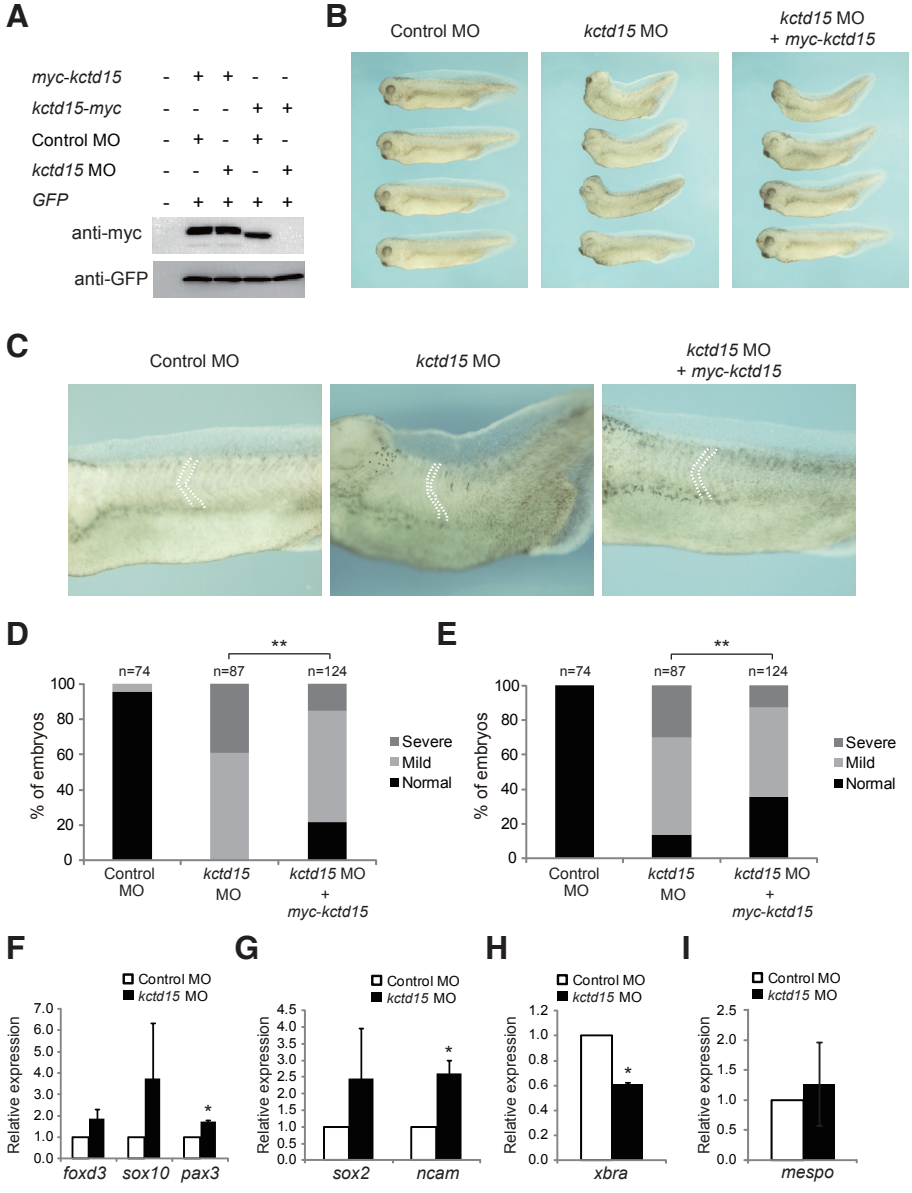

Fig. 4. Essential role of *Xenopus kctd15* in dorsal development. (A) *The specificity and efficiency of* kctd15 *MO. The combination of* GFP *mRNA (200 pg) plus control MO (80 ng) or* kctd15 *MO (80 ng) was co-injected with* myc-kctd15 *(800 pg) or* kctd15-myc *mRNA (800 pg) into* Xenopus *embryos. Injected embryos were harvested for immunoblotting at stage 10.5.* **(B,C)** *Control MO (80 ng) or* kctd15 *MO (80 ng) was injected into the animal pole of each dorsal blastomere at the four-cell stage. For rescue experiments,* myc-kctd15 *mRNA (800 pg) was coinjected with* kctd15 *MO (80 ng). At the late tailbud stage, injected embryos were photographed with anterior to the left and dorsal to the top. White dotted lines in C represent somite boundaries.* **(D)** *Obtained phenotypes were classified into three groups (severe, mild or normal) according to the extent of defects in head morphologies. **, P < 0.01. Fisher's exact test was used to compare the frequency of normal head development between embryos injected with* kctd15 *MO alone and those injected with* kctd15 *MO plus* myc-kctd15 *mRNA. P = 6.5 x* 10^{-8}. **(E)** *Obtained phenotypes were classified into three groups (severe, mild or normal) according to the extent of defects in somite morphologies. **, P < 0.01. Fisher's exact test was used to compare the frequency of normal somite development between embryos injected with* kctd15 *MO alone and those injected with* kctd15 *MO plus* myc-kctd15 *mRNA. P = 0.00045.* **(F-I)** *Real-time quantitative RT–PCR analysis of marker gene expression. Embryos dorsally injected with control MO (80 ng) or* kctd15 *MO (80 ng) were cultured until stage 15 (F, G) or 19 (H, I). The relative expression levels of the indicated genes were normalized to that of* odc. *Shown is the average of two (F-H) or four (I) independent experiments. The error bar represents SD. *P < 0.05, **P < 0.01, unpaired t test. P values versus control were as follows: 0.11 for* foxd3 *expression, 0.27 for* sox10 *expression, 0.0046 for* pax3 *expression, 0.31 for* sox2 *expression, 0.029 for* ncam *expression, 0.00083 for* xbra *expression, and 0.47 for* mespo *expression.*

anteroposterior width of each somitic unit, 56% of those showed milder phenotypes with the normal dorsoventral length but the decreased anteroposterior width of each somitic unit, and only 14% of those had normal somites (Fig. 4E). Next, to confirm the specificity of *kctd15* MO, we performed rescue experiments with an N-terminally myc-tagged *kctd15* (*myc-kctd15*), which contains the full-length coding sequence but not the 5'UTR. *Kctd15* MO did not suppress the protein abundance of myc-kctd15 (Fig. 4A, lanes 2 and 3), indicating that *myc-kctd15* is a *kctd15* MO-resistant construct. We then examined whether co-injection of *myc-kctd15* mRNA rescues the phenotype induced by *kctd15* MO (Fig. 4 B-E). When coinjected, the percentage of embryos with severe defects in head morphologies was decreased to 15%, while the percentage of those with normal heads was increased to 22%. Also, defects in somite morphologies were partially rescued by coinjection: the percentage of embryos with severe defects was decreased to 13%, while the percentage of those with normal somites was increased to 35%. The observed phenotypes in *kctd15* morphants are thus largely due to the depletion of kctd15 protein.

We next performed real-time quantitative RT-PCR analysis to elucidate a molecular basis for these phenotypes. Because *kctd15* is expressed in the neural plate border including the neural crest (Fig. 2), we first examined the expression levels of the neural plate border specifier, *pax3*, and neural crest markers, *foxd3* and *sox10*. At the mid-neurula stage (stage 15), dorsal injection of *kctd15* MO led to a slight or moderate increase in expression of *foxd3*, *sox10* and *pax3* (Fig. 4F). Moreover, the expression levels of neural markers, *sox2* and *ncam*, were also increased by *kctd15* MO (Fig. 4G). These results suggest that dorsal depletion of kctd15 leads to hyperplasia of neural crest and neural tissues. Also, we analyzed the expression level of *xbra*, which is required for somite formation (Conlon *et al.*, 1996). *Xbra* expression at the late neurula stage (stage 19) was reduced to about 60% by *kctd15* MO (Fig. 5H), suggesting the possibility that somitic defects caused by kctd15 depletion are partly due to downregulation of *xbra*. By contrast, dorsal depletion of kctd15 did not significantly affect the expression level of the bHLH transcription factor *mesogenin1*/*mespo*, a major Wnt/beta-catenin target gene critical for somite segmentation (Wang *et al.*, 2007, Chalamalasetty *et al.*, 2011), at stage 19 (Fig. 4I). Thus, dysregulation of Wnt/beta-catenin signaling during somitogenesis might not be primarily responsible for somatic defects caused by kctd15 depletion.

Xenopus Kctd15 *is essential for ventral and caudal development*

Next, *kctd15* MO was injected into animal poles of ventral blastomeres at the four-cell stage. At the late tailbud stage, injected embryos exhibited defects in ventral and caudal morphologies (Fig. 5A). Thirty-four percent of *kctd15* MO-injected embryos showed severe phenotypes with poorly extended tails and reduced ventral tissues, 36% of those showed milder phenotypes with poorly extended tails but the relatively normal ventral morphology, and 30% of those showed no phenotypes (Fig. 5B). Coinjection of *myc-kctd15* mRNA rescued the phenotype induced by *kctd15* MO: eleven percent of coinjected embryos showed severe phenotypes, 17% of those showed mild phenotypes, and 71% of those had no phenotypes (Fig. 5B). The observed phenotypes in *kctd15* morphants are thus largely due to ventral depletion of kctd15.

The expression levels of marker genes were also examined by real-time quantitative RT-PCR analysis. Ventral injection of *kctd15*

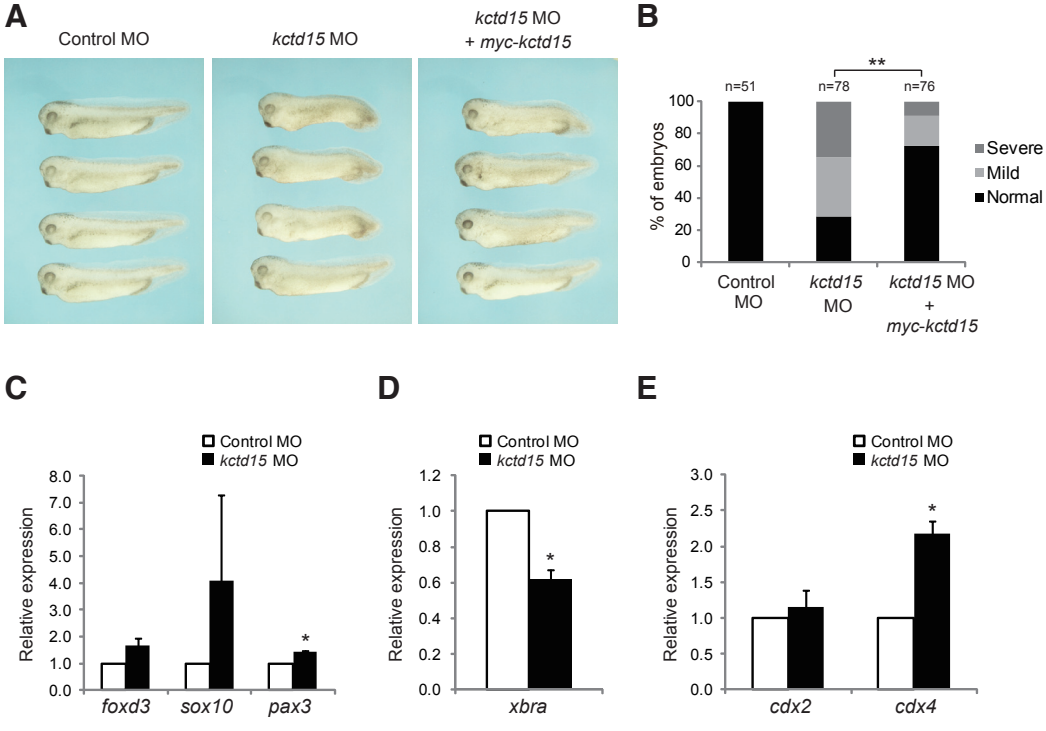

Fig. 5. Essential role of *Xenopus kctd15* in ventral development. (A) *Control MO (80 ng) or* kctd15 *MO (80 ng) was injected into the animal pole of each ventral blastomere at the four-cell stage. For rescue experiments,* myc-kctd15 *mRNA (700 pg) was coinjected with* kctd15 *MO (80 ng). At the late tailbud stage, injected embryos were photographed with anterior to the left and dorsal to the top.* **(B)** *Obtained phenotypes were classified into three groups (severe, mild or normal) according to the extent of defects in ventral and caudal morphologies. **, P < 0.01. Fisher's exact test was used to compare the frequency of normal development between embryos injected with* kctd15 *MO alone and those injected with* kctd15 *MO plus* myc-kctd15 *mRNA. P = 2.7 x* 10^{-5}. **(C-E)** *Real-time quantitative RT-PCR analysis of marker gene expression. Embryos ventrally injected with control MO (80 ng) or* kctd15 *MO (80 ng) were cultured until stage 15 (C), 19 (D) or 24 (E). The relative expression levels of the indicated genes were normalized to that of* odc. *Shown is the average of two independent experiments. The error bar represents SD. *P < 0.05, **P < 0.01, unpaired t test. P values versus control were as follows: 0.085 for* foxd3 *expression, 0.30 for* sox10 *expression, 0.00065 for* pax3 *expression, 0.0089 for* xbra *expression, and 0.48 for* cdx2 *expression, and 0.011 for* cdx4 *expression.*

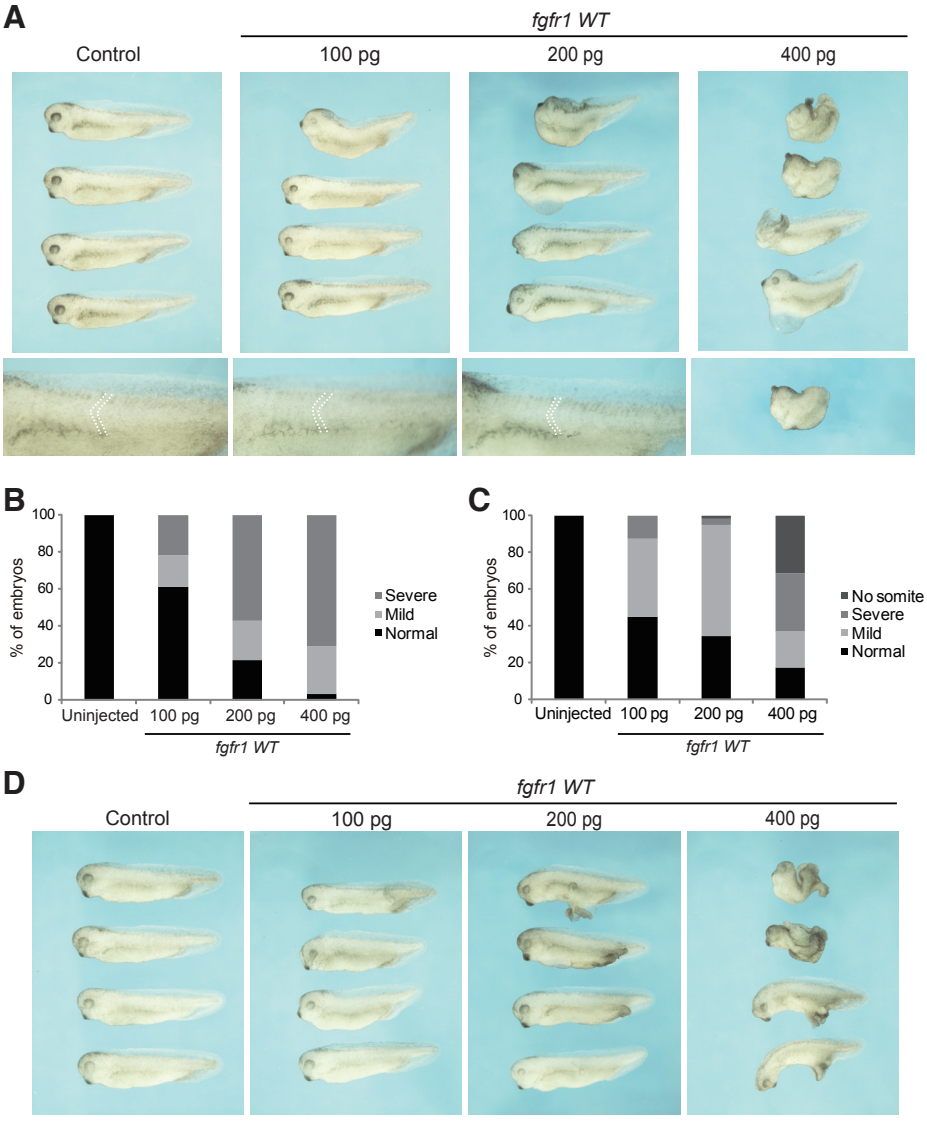

Fig. 6. Ectopic dorsal expression of *fgfr1* phenocopies dorsal depletion of *Xenopus* kctd15. (A) *The indicated dose of* fgfr1 WT *mRNA was injected into the animal pole of each dorsal blastomere at the four-cell stage. Embryos were photographed at the late tailbud stage.* **(B)** *Obtained phenotypes were classified into three groups (severe, mild or normal) according to the extent of defects in head morphologies.* **(C)** *Obtained phenotypes were classified into four groups (no somite, severe, mild or normal) according to the extent of defects in somite formation.* **(D)** *The indicated dose of* fgfr1 WT *mRNA was injected into the animal pole of each ventral blastomere at the four-cell stage. Embryos were photographed at the late tailbud stage.*

MO led to a weak increase in expression of neural crest markers at the mid-neurula stage (stage 15) (Fig. 5C). Also, at the late neurula stage (stage 19), the expression level of *xbra*, which is important for posterior mesoderm formation in addition to somite formation (Conlon *et al.*, 1996), was decreased by ventral depletion of kctd15 (Fig. 5D). We also focused on caudal type homeobox transcription factors, *cdx2* and *cdx4*, which are important for posterior axial elongation (Mallo *et al.*, 2010). The expression level of *cdx4* at the early tailbud stage (stage 24), but not that of *cdx2*, was increased by ventral depletion of kctd15 (Fig. 5E). These changes in gene expression may potentially contribute to defects in ventral or caudal morphologies observed in embryos ventrally injected with *kctd15* MO.

Dorsal activation of FGF signaling partially phenocopies dorsal depletion of Xenopus *kctd15*

Finally, to test whether the FGF pathway is related to phenotypes observed in *kctd15* morphants, wild-type *Xenopus FGF receptor 1* (*fgfr1 WT*) mRNA was injected into animal poles of dorsal or ventral blastomeres at the four-cell stage. At the late tailbud stage, embryos dorsally injected with 100 or 200 pg of *fgfr1 WT* mRNA showed similar defects in head and somite development to those observed in embryos dorsally injected with *kctd15* MO (Fig. 6 A-C). Embryos dorsally injected with 400 pg of *fgfr1 WT* mRNA showed much severer defects including spina bifida (Fig. 6 A-C), which was not observed in *kctd15* morphants (Fig. 4B). These data suggest that moderate activation of FGF signaling in the dorsal halves of embryos partially phenocopies dorsal depletion of kctd15. Meanwhile, embryos ventrally injected with 100 pg or 200 pg of *fgfr1 WT* mRNA showed normal tail extension with or without ectopic posterior protrusions, while those ventrally injected with 400 pg of *fgfr1 WT* mRNA showed truncated anteroposterior axes or ectopic posterior protrusions (Fig. 6D). These phenotypes were not observed in embryos ventrally injected with *kctd15* MO (Fig. 5A), suggesting that ventral activation of FGF signaling does not phenocopy ventral depletion of kctd15. Taken together, downregulation of *kctd15* expression may partly mediate the action of FGF signaling in a context-dependent manner.

Discussion

In this study, we have identified *Xenopus kctd15* as an FGF-repressed gene. *Kctd15* is not maternally expressed, and its zygotic transcription begins during gastrulation. While *kctd15* is uniformly expressed throughout the presumptive ectoderm at the early gastrula stage, its expression becomes restricted to the non-neural ectoderm at the early neurula stage. At mid- to late neurula stages, *kctd15* shows a more restricted distribution pattern in the prospective neural crest, the preplacodal ectoderm and the prospective roof plate. At the tailbud stage, *kctd15* expression is mainly detected in neural crest- or placode-derived tissues surrounding the eye. Dorsal depletion of kctd15 in *Xenopus* embryos leads to bent axes with reduced head structures, defective eyes and abnormal somites, while ventral depletion causes defects in ventral and caudal morphologies. These results thus suggest that *Xenopus kctd15* plays a crucial role in early embryonic development.

The recent study showed the spatial expression pattern of two zebrafish *KCTD15* orthologs, *kctd15a* and *kctd15b* (Dutta and Da-

wid, 2010). At the 1-somite stage, both genes are mainly expressed in the neural plate border. At later stages, zebrafish *kctd15a* is mainly expressed in pronephric ducts, cranial placode precursors and the brain, while zebrafish *kctd15b* is mainly expressed in the olfactory placode, the cranial neural crest, pharyngeal arches, fin buds and the optic tectum. Thus, the expression pattern of zebrafish *kctd15a/b* is not identical to, but overlaps with, that of *Xenopus kctd15*. It has also been shown that zebrafish embryos injected with MOs against *kctd15a* and *kctd15b* exhibit small heads and abnormal somites (Dutta and Dawid, 2010). These phenotypes are very similar to those observed in *Xenopus* embryos dorsally injected with *kctd15* MO (Fig. 4). It can be therefore assumed that the function of KCTD15 in dorsal development is conserved in both zebrafish and *Xenopus*.

Our results also showed that ventral depletion of *Xenopus* kctd15 causes defects in ventral and caudal morphologies, including poorly extended tails and reduced ventral tissues (Fig. 5). Although the previous study in zebrafish did not mention ventral and caudal morphologies in embryos depleted of both Kctd15a and Kctd15b, poorly extended tails seem to be observed in morphants (see Fig. 1J-M in Dutta and Dawid, 2010). Therefore, the function of KCTD15 in caudal development may be conserved in both zebrafish and *Xenopus*. Further analyses in other vertebrates are necessary to demonstrate an evolutionary conservation of KCTD15 function in development.

What mechanisms could be responsible for the observed phenotypes in *Xenopus* embryos depleted of kctd15? Our quantitative RT-PCR results showed that dorsal depletion of kctd15 leads to an increase in expression of neural crest and neural markers (Fig. 4). Because the previous study in zebrafish has shown that knockdown of both *kctd15a* and *kctd15b* leads to the expansion of the neural crest (Dutta and Dawid, 2010), malformation of the cranial neural crest would be a primary cause of defects in head morphologies induced by dorsal injection of *kctd15* MO. Hyperplasia of neural tissues could be an additional potential cause. Also, dorsal depletion of kctd15 leads to a decrease in expression of *xbra* (Fig. 4). *Xbra* and its homologs (zebrafish *no tail* and mouse *Brachyury*) are implicated in somite formation (Wardle and Papaioannou, 2008). Thus, downregulation of *xbra* expression may be relevant to defects in somite morphologies.

Our quantitative RT-PCR results also reveal that ventral depletion of *Xenopus* kctd15 caused an increase in *cdx4* expression and a decrease in *xbra* expression (Fig. 5). *Xenopus* embryos ventrally injected with *cdx4* mRNA had poorly extended tails, although the authors did not mention it (see Fig. 7H in Pownall *et al.*, 1996). Moreover, *xbra* homologs are required for tail formation in vertebrates including zebrafish, *Xenopus* and mouse (Wardle and Papaioannou, 2008). Thus, changes in *cdx4* and *xbra* expression may be primarily responsible for the defects in caudal morphologies observed in *Xenopus* embryos ventrally injected with *kctd15* MO. Because ventral depletion of kctd15 also leads to a slight increase in expression of neural crest markers (Fig. 5), excess neural crest-derived tissues in the ventral region could be an additional potential cause. Because *Xenopus kctd15* shows a characteristic expression pattern in various tissues (Fig. 2), other multiple factors in addition to those described above also might contribute to the phenotypes of *kctd15* knockdown embryos.

The interplay between the FGF and Wnt signaling pathways regulates a variety of developmental processes (Dailey *et al.*, 2005). In the previous study, KCTD15 has been shown to antagonize the canonical Wnt pathway (Dutta and Dawid, 2010). Because we have here identified *Xenopus kctd15* as an FGF/Ras-repressed gene, it can be speculated that the FGF/Ras pathway indirectly promotes the Wnt pathway by repressing *kctd15* expression. Our results of whole-mount *in situ* hybridization definitely indicate that FGF-mediated transcriptional repression of *kctd15* contributes to the region-specific expression of *kctd15*, which might result in the region-specific activation or repression of Wnt signaling that is responsible for proper embryonic development. We recently reported that another Ras-repressed gene, *eig121l*, is specifically expressed in the ventral ectoderm and acts as a positive regulator of the BMP pathway (Araki *et al.*, 2007; Araki *et al.*, 2011). Thus, FGF/Ras-induced transcriptional repression of signaling molecules may represent a mechanism mediating the crosstalk among multiple signaling pathways.

Materials and Methods

Molecular cloning and plasmid construction

The full-length of *Xenopus kctd15* was already deposited in GenBank (GenBank accession number BC077862). We designed primers on the basis of the deposited sequences, and performed RT-PCR with complementary DNAs (cDNAs) derived from embryos at stage 12. The amplified entire coding sequence was cloned into the pBluescript vector for RNA probe synthesis.

Embryo manipulations

Xenopus laevis embryos were obtained by *in vitro* fertilization and cultured in 0.1 x MBS (1.0 mM HEPES, pH 7.4, 8.8 mM NaCl, 0.1 mM KCl, 0.24 mM $NaHCO_3$, 0.082 mM $MgSO_4$, 0.03 mM $Ca(NO_3)_2$ and 0.041 mM $CaCl_2$). Embryos were staged according to Nieuwkoop and Faber (Nieuwkoop and Faber, 1967). Injection of embryos was performed in 4% Ficoll in 0.1 x MBS. For animal cap assay, human *RasV12* mRNA was injected into animal poles of four-cell stage embryos. Ectodermal explants were dissected at stage 8 (Fig. 1A) or 10.25 (Fig. 3A) and cultured in 1 x Steinberg's solution (10 mM Hepes, pH 7.4, 60 mM NaCl, 0.67 mM KCl, 0.83 mM $MgSO_4$ and 0.34 mM $Ca(NO_3)_2$) containing 1 mg/ml BSA (Sigma). The explants were harvested at indicated stages for RT-PCR. For the whole embryo phenotypes, antisense morpholino oligonucleotides (MOs) were injected into animal poles of two dorsal or ventral blastomeres at the four-cell stage (40 ng of each MO per blastomere). The injected embryos were cultured in 4% Ficoll in 0.1 x MBS until stage 9, and then transferred to 0.1 x MBS.

Quantitative reverse transcription-PCR

Total RNA was extracted from whole embryos or animal caps using TRIzol reagent (Invitrogen). cDNA was synthesized using M-MLV reverse transcriptase (Invitrogen). For real-time quantitative RT-PCR analysis, we used 7300 real-time PCR System (Applied Biosystems) with SYBR Green PCR Master Mix (QIAGEN). The primers for *ef1a* have been previously described (Gotoh *et al.*, 1995). The other sequences of primer pairs used were as follows:

odc	forward 5'-TGCAAGTTGGAGACTGGATG
	reverse 5'-CATCAGTTGCCAGTGTGGTC
kctd15	forward 1 (f1) 5'-ATTGCTCTAAGCGGAGAAAAGG
	forward 2 (f2) 5'-TGGCTGCCCAAGGAATACCTCTTCC
	reverse 1 (r1) 5'-ACTAAACTGCGAGGAGTCAACG
	reverse 2 (r2) 5'-ACTTTGTCAGGGTGGCCAGACTGC
foxd3	forward 5'-CCTGTCAGGCAGCGGCAGTG
	reverse 5'-CTTGTCCAGCGCCTCGTCCC
sox10	forward 5'-AGAGGAGGCTGAGAGGCTGCG
	reverse 5'-ACCCTCGGCTTCAGAGGACCC
pax3	forward 5'-AGCAGCGCAGGAGCAGAACC

	reverse 5'-ACCACACCTGAACTCGCGCC
sox2	forward 5'-GGCAGAAGTGCCAGAGTCCGC
	reverse 5'-ATGTGCGACAGAGGCAGCGTG
ncam	forward 5'-CAGATTCCACTGGTGGTGTG
	reverse 5'-TGATGCTCTCTGCATTCACC
xbra	forward 5'-GCTGGAAGTATGTGAATGGAG
	reverse 5'-TTAAGTGCTGTAATCTCTTCA
mespo	forward 5'-TGAGGCCCTTCATACCCTCCGC
	reverse 5'-GCTGATGGTGCACTTCAAGGTTTGG
cdx2	forward 5'-CGGCGCAGGTGCAAGGACAG
	reverse 5'-CGTAGTGATGCCGCCGGTGTTC
cdx4	forward 5'-CCAAACCCACTTTGTGACTCTGCGG
	reverse 5'-GCTTGCAGACACTTCCAGCTCTTGC.

Kctd15-f1 and *kctd15*-r1 primers were used in Fig. 1A. *Kctd15*-f2 and *kctd15*-r2 primers were used in Figures 1E and 3.

Whole-mount in situ *hybridization*

Whole-mount *in situ* hybridization on albino *Xenopus* embryos was performed according to the standard protocol (Sive *et al.*, 2000), using a robot (InsituPro, Intavis). The digoxygenin-labeled antisense and sense probes were synthesized from cDNA corresponding to the coding region of *Xenopus kctd15*. For single *in situ* hybridization, color reactions were performed using BM purple or NBT/BCIP alkaline phosphatase substrate (Roche). For double *in situ* hybridization, the first color reaction for the digoxygenin-labeled *kctd15* probe was performed using BM purple. To inactivate remaining alkaline phosphatase derived from the first reaction, stained embryos were washed with PBS (pH 5.5) containing 5 mM EDTA, and refixed with 4% paraformaldehyde in PBS for overnight. The second color reaction for the fluorescein-labeled *sox10* probe was performed in a solution containing INT/BCIP (Roche) and 5% polyvinyl alcohol.

Morpholino oligonucleotides

Antisense morpholino oligonucleotides were obtained from Gene Tools Inc. The MO sequences were as follows: *Xenopus kctd15* MO, 5'-TTA GAG ACA GAC GGG ACA TTT TGC T-3'; a standard control oligo (control MO), 5'-CCT CTT ACC TCA GTT ACA ATT TAT A-3'. Sequences complementary to the predicted start codon are underlined. These MOs were resuspended in sterile water.

Immunoblotting

Embryos were lysed in a buffer consisting of 20 mM HEPES (pH 7.2), 0.25 M sucrose, 0.1 M NaCl, 2.5 mM $MgCl_2$, 10 mM NaF, 10 mM EGTA, 10 mM β-glycerophosphate, 1 mM vanadate, 1 mM phenylmethylsulfonyl fluoride, 0.5% aprotinin, and 1 mM dithiothreitol. The lysate was centrifuged and the supernatant was used for immunoblotting with an antibody against Myc (9E10; Santa Cruz Biotechnology).

Acknowledgements

We thank T. Araki and K. Miyatake for technical advice and helpful discussion. This work was supported by grants from the Ministry of Education, Culture, Sports, Science and Technology of Japan (to E.N. and M.K.) and CREST, JST (to E.N.). T.S. is a research fellow of the Japan Society for the Promotion of Science.

References

AMAYA, E., MUSCI, T. J. and KIRSCHNER, M. W. (1991). Expression of a dominant negative mutant of the FGF receptor disrupts mesoderm formation in *Xenopus* embryos. *Cell* 66: 257-270.

ARAKI, T., KUSAKABE, M. and NISHIDA, E. (2007). Expression of estrogen induced gene 121-like (EIG121L) during early *Xenopus* development. *Gene Expr Patterns* 7: 666-671.

ARAKI, T., KUSAKABE, M. and NISHIDA, E. (2011). A transmembrane protein EIG121L is required for epidermal differentiation during early embryonic development. *J Biol Chem* 286: 6760-6768.

BARTOI, T., RIGBOLT, K. T., DU, D., KÖHR, G., BLAGOEV, B. and KORNAU, H. C. (2010). GABAB receptor constituents revealed by tandem affinity purification from transgenic mice. *J Biol Chem* 285: 20625-20633.

BÖTTCHER, R. T. and NIEHRS, C. (2005). Fibroblast growth factor signaling during early vertebrate development. *Endocr Rev* 26: 63-77.

BRANNEY, P. A., FAAS, L., STEANE, S. E., POWNALL, M. E. and ISAACS, H. V. (2009). Characterisation of the fibroblast growth factor dependent transcriptome in early development. *PLoS One* 4: e4951.

CANETTIERI, G., DI MARCOTULLIO, L., GRECO, A., CONI, S., ANTONUCCI, L., INFANTE, P., PIETROSANTI, L., DE SMAELE, E., FERRETTI, E., MIELE, E. *et al.*, (2010). Histone deacetylase and cullin3-REN(KCTD11) ubiquitin ligase interplay regulates hedgehog signalling through Gli acetylation. *Nat Cell Biol* 12: 132-142.

CHALAMALASETTY, R. B., DUNTY, W. C. JR., BIRIS, K. K., AJIMA, R., IACOVINO, M., BEISAW, A., FEIGENBAUM, L., CHAPMAN, D. L., YOON, J. K., KYBA, M. and YAMAGUCHI, T. P. (2011). The Wnt3a/β-catenin target gene Mesogenin1 controls the segmentation clock by activating a Notch signalling program. *Nat Commun* 2: 390.

CHUNG, H. A., HYODO-MIURA, J., KITAYAMA, A., TERASAKA, C., NAGAMUNE, T. and UENO, N. (2004). Screening of FGF target genes in *Xenopus* by microarray: temporal dissection of the signalling pathway using a chemical inhibitor. *Genes Cells* 9: 749-761.

CONLON, F. L., SEDGWICK, S. G., WESTON, K. M. and SMITH, J. C. (1996). Inhibition of Xbra transcription activation causes defects in mesodermal patterning and reveals autoregulation of Xbra in dorsal mesoderm. *Development* 122: 2427-2435.

DAILEY, L., AMBROSETTI, D., MANSUKHANI, A. and BASILICO, C. (2005). Mechanisms underlying differential responses to FGF signaling. *Cytokine Growth Factor Rev* 16: 233-247.

DE ROBERTIS, E. M. and KURODA, H. (2004). Dorsal-ventral patterning and neural induction in *Xenopus* embryos. *Annu Rev Cell Dev Biol* 20: 285-308.

DI MARCOTULLIO, L., FERRETTI, E., DE SMAELE, E., ARGENTI, B., MINCIONE, C., ZAZZERONI, F., GALLO, R., MASUELLI, L., NAPOLITANO, M., MARODER, M. *et al.,* (2004). REN(KCTD11) is a suppressor of hedgehog signaling and is deleted in human medulloblastoma. *Proc Natl Acad Sci USA* 101: 10833-10838.

DUTTA, S. and DAWID, I. B. (2010). Kctd15 inhibits neural crest formation by attenuating Wnt/beta-catenin signaling output. *Development* 137: 3013-3018.

GOTOH, Y., MASUYAMA, N., SUZUKI, A., UENO, N. and NISHIDA, E. (1995). Involvement of the MAP kinase cascade in *Xenopus* mesoderm induction. *EMBO J* 14: 2491-2498.

HEASMAN, J. (2006). Patterning the early *Xenopus* embryo. *Development* 133: 1205-1217.

MALLO, M., WELLIK, D. M. and DESCHAMPS, J. (2010). Hox genes and regional patterning of the vertebrate body plan. *Dev Biol* 344: 7-15.

NIEUWKOOP, P. D. and FABER, J. (1967). Normal table of *Xenopus laevis* (*Daudin*). North Holland Publishing Co, Amsterdam.

PEREZ-TORRADO, R., YAMADA, D. and DEFOSSEZ, P. A. (2006). Born to bind: The BTB protein-protein interaction domain. *Bioessays* 28: 1194-1202.

POWNALL, M. E., TUCKER, A. S., SLACK, J. M. and ISAACS, H. V. (1996). eFGF, Xcad3 and Hox genes form a molecular pathway that establishes the anteroposterior axis in *Xenopus. Development* 122: 3881-3892.

SADAGHIANI, B. and THIÉBAUD, C. H. (1987). Neural crest development in the *Xenopus laevis* embryo, studied by interspecific transplantation and scanning electron microscopy. *Dev Biol* 124: 91-110.

SCHWENK, J., METZ, M., ZOLLES, G., TURECEK, R., FRITZIUS, T., BILDL, W., TARUSAWA, E., KULIK, A., UNGER, A., IVANKOVA, K. *et al.*, (2010). Native GABA(B) receptors are heteromultimers with a family of auxiliary subunits. *Nature* 465: 231-235.

SMITH, J. C., PRICE, B. M., GREEN, J. B., WEIGEL, D. and HERRMANN, B. G. (1991). Expression of a *Xenopus* homolog of *Brachyury (T)* is an immediate-early response to mesoderm induction. *Cell* 67: 79-87.

SIVE, H. L., GRAINGER, R. M. and HARLAND, R. M. (2000). Early development of *Xenopus laevis*: A laboratory manual. Cold Spring Harbor Laboratory Press, Cold Spring Harbor, NY.

THISSE, B. and THISSE, C. (2005). Functions and regulations of fibroblast growth factor signaling during embryonic development. *Dev Biol* 287: 390-402.

THORLEIFSSON, G., WALTERS, G. B., GUDBJARTSSON, D. F., STEINTHORS-

DOTTIR, V., SULEM, P., HELGADOTTIR, A., STYRKARSDOTTIR, U., GRETARSDOTTIR, S., THORLACIUS, S., JONSDOTTIR, I. *et al.*, (2009). Genome-wide association yields new sequence variants at seven loci that associate with measures of obesity. *Nat Genet* 41: 18-24.

WANG, J., LI, S., CHEN, Y. and DING, X. (2007). Wnt/beta-catenin signaling controls Mespo expression to regulate segmentation during *Xenopus* somitogenesis. *Dev Biol* 304: 836-847.

WARDLE, F. C. and PAPAIOANNOU, V. E. (2008). Teasing out T-box targets in early mesoderm. *Curr Opin Genet Dev* 18: 418-425.

WILLER, C. J., SPELIOTES, E. K., LOOS, R. J., LI, S., LINDGREN, C. M., HEID, I. M., BERNDT, S. I., ELLIOTT, A. L., JACKSON, A. U., LAMINA, C. *et al.*, (2009). Six new loci associated with body mass index highlight a neuronal influence on body weight regulation. *Nat Genet* 41: 25-34.

Further Related Reading, published previously in the *Int. J. Dev. Biol.*

Pluripotency of bank vole embryonic cells depends on FGF2 and activin A signaling pathways
Aneta Suwinska, Andrzej K. Tarkowski and Maria A. Ciemerych
Int. J. Dev. Biol. (2010) 54: 113-124

Expression of Shisa2, a modulator of both Wnt and Fgf signaling, in the chick embryo
Thomas A. Hedge and Ivor Mason
Int. J. Dev. Biol. (2008) 52: 81-85

Expression of the novel gene Ened during mouse and Xenopus embryonic development
Renata Meszaros, Ina Strate, Edgar M. Pera and Madeleine Durbeej
Int. J. Dev. Biol. (2008) 52: 1119-1122

The preplacodal region: an ectodermal domain with multipotential progenitors that contribute to sense organs and cranial sensory ganglia
Andrea Streit
Int. J. Dev. Biol. (2007) 51: 447-461

Fibroblast growth factor signalling and regional specification of the pharyngeal ectoderm
Nina Trokovic, Ras Trokovic and Juha Partanen
Int. J. Dev. Biol. (2005) 49: 797-805

Spemann's influence on Japanese developmental biology
M Asashima and T S Okada
Int. J. Dev. Biol. (2001) 45: 57-65

Evidence for non-axial A/P patterning in the nonneural ectoderm of Xenopus and zebrafish pregastrula embryos
E M Read, A R Rodaway, B Neave, N Brandon, N Holder, R K Patient and M E Walmsley
Int. J. Dev. Biol. (1998) 42: 763-774

5 yr ISI Impact Factor (2010) = 2.961